FERMILAB-PUB-82-109-E Submitted to
Z Phys. C, 5/18/82

The reactions $pp \to pp\pi^+\pi^-$, $K^+p \to K^+p\pi^+\pi^-$, $\pi^+p \to \pi^+p\pi^+\pi^-$ and $\pi^-p \to \pi^-p\pi^+\pi^-$ at 147 GeV/c

D. H. Brick, H. Rudnicka, A. M. Shapiro, M. Widgoff
Brown University, Providence, Rhode Island 02912

R. E. Ansorge, W. W. Neale, D. R. Ward, B. M. Whyman[a]
University of Cambridge, Cambridge, England

R. A. Burnstein, H. A. Rubin
Illinois Institute of Technology, Chicago, Illinois 60616

E. D. Alyea, Jr.
Indiana University, Bloomington, Indiana 47401

L. Bachman[b], C.-Y. Chien, P. Lucas[c], A. Pevsner
Johns Hopkins University, Baltimore, Maryland 21218

J. T. Bober, R. Dolfini[d], T. A. J. Frank, E. S. Hafen, P. Haridas, D. Huang[e],
R. I. Hulsizer, V. Kistiakowsky, P. Lutz[f], S. Noguchi[g], S. H. Oh,
I. A. Pless, T. B. Stoughton, V. Suchorebrow, S. Tether,
P. C. Trepagnier[h], Y. Wu[e], R. K. Yamamoto
Laboratory for Nuclear Science and Department of Physics
Massachusetts Institute of Technology, Cambridge, Massachusetts 02139

F. Grard, J. Hanton, V. Henri, P. Herquet, J. M. Lesceux,
P. Pilette, R. Windmolders
Université de l'Etat, Mons, Belgium

H. de Bock[i], F. Crijns, W. Kittel, W. Metzger, C. Pols,
M. Schouten[j], R. Van de Walle
University of Nijmegen and NIKHEF-H, Nijmegen, The Netherlands

H. O. Cohn
Oak Ridge National Laboratory, Oak Ridge, Tennessee 37830

G. Bressi, E. Calligarich, C. Castoldi, S. Ratti
Istituto di Fisica Nucleare and Sezione INFN, Pavia, Italy

R. DiMarco, P. F. Jacques, M. Kalelkar, R. J. Plano,
P. E. Stamer[k], T. L. Watts
Rutgers University, New Brunswick, New Jersey 08903

E. B. Brucker, E. L. Koller, S. Taylor
Stevens Institute of Technology, Hoboken, New Jersey 07030

L. Berny, S. Dado, J. Goldberg, S. Toaff
Technion, Haifa, Israel 32000

G. Alexander, O. Benary, J. Grunhaus, R. Heifetz, A. Levy
Tel Aviv University, Ramat-Aviv, Israel 69978

W. M. Bugg, G. T. Condo, T. Handler, E. L. Hart, A. H. Rogers
University of Tennessee, Knoxville, Tennessee 37830

Y. Eisenberg, D. Hochman, U. Karshon, E. E. Ronat,
A. Shapira, R. Yaari, G. Yekutieli
Weizmann Institute of Science, Rehovot, Israel

T. W. Ludlam[1], R. V. Steiner, H. D. Taft
Yale University, New Haven, Connecticut 06520

Abstract

We have studied the reactions $pp \to pp\,\pi^+\pi^-$, $K^+p \to K^+p\,\pi^+\pi^-$, $\pi^+p \to \pi^+p\,\pi^+\pi^-$, and $\pi^-p \to \pi^-p\,\pi^+\pi^-$ at 147 GeV/c using the 30-inch Fermilab hybrid system. All four reactions were detected with the same apparatus and analyzed in the same way. The energy dependence of the channel cross section was found to be $Ap^{-0.6}+B$ for the pp reaction and $Ap^{-1}+B$ for the other three ones. About 90% of the cross section at 147 GeV/c can be accounted for by either beam or target diffraction. Some of the remaining cross section may come from double Pomeron exchange reactions which we tried to isolate. We show that the 3π mass enhancement in the A_2 mass region is diffractively produced in the $\pi^{\pm}$ beam reactions, in violation of the Gribov-Morrison rule.

I. Introduction

Reactions of the type $a+p \rightarrow a + p + \pi^+ + \pi^-$, where a is the beam particle, can be accounted for by two types of mechanisms: one involving the exchange of a single particle (Figs. 1(a), 1(b) and 1(c)), and one in which two particles are exchanged (Figs. 1(d), 1(e), and 1(f)). At high energies, one expects the single exchange processes to be dominated by the Pomeron and the main contributions would come from diffraction of either the beam a into a $(a\pi^+\pi^-)$ system or the target p into a $(p\pi^+\pi^-)$ system. In a π^-p experiment at 147 GeV/c, it was shown that about 90% of the channel cross section is contained in those for proton and pion diffraction dissociation [1]. The same has been shown to be true in a π^-p experiment at 205 GeV/c [2]. Some information also exists on reactions proceeding via the diagram shown in fig. 1(f), where the beam projectile and the target particle both emit a Pomeron,and the remaining $\pi^+\pi^-$ are centrally produced via the two-Pomeron interaction (Double Pomeron Exchange - DPE) [3]. The DPE reactions could be a possible mechanism for glueball production [4].

In this publication, we analyze the four reactions

$$pp \rightarrow pp\ \pi^+\pi^- \qquad (1)$$

$$K^+p \rightarrow K^+p\ \pi^+\pi^- \qquad (2)$$

$$\pi^+p \rightarrow \pi^+p\ \pi^+\pi^- \qquad (3)$$

$$\pi^-p \rightarrow \pi^-p\ \pi^+\pi^- \qquad (4)$$

at 147 GeV/c beam momentum. All four reactions have been measured using the same apparatus and the same data handling procedures. The experimental details are presented in Section II. The cross sections for reactions (1) - (4) are given in Section III, where we also discuss their energy dependence. Section IV contains

information about the diffraction of the beam projectile or of the target particle. The DPE reaction is discussed in Section V. Section VI includes a comparison of the π^+ and π^- beam diffraction into a (3π) low-mass enhancement. The results are summarized and conclusions given in Section VII.

II. Experimental details

The data used in the present study come from two exposures in the Fermilab 30-inch hybrid spectrometer: one with a tagged negative beam, mainly π^-, and one with a tagged positive beam, composed of π^+, K^+, and p. Beam particle identification was made by a threshold and differential Čerenkov counter. In both exposures, the beam momentum was 147 GeV/c. The results of the 105,000 picture π^-p exposure have already been published [1, 5]. The 400,000 picture, positive-beam exposure consisted of two parts: one in which the beam content was mainly π^+ and p with a very small number of K^+'s, and another with the ratio of $\pi^+/K^+/p$ of 6/1/3. A small prototype of a lead-glass forward gamma detector was added for the second part of the positive exposure. Details of the experimental arrangement and of the data reduction have already been published [6].

The present study is based on 299 events of reaction (1), 38 events of reaction (2), 487 of reaction (3), and 348 events of reaction (4). These events have been obtained by performing 4-constraint (4-C) fits with the kinematic fitting program SQUAW modified for ultrarelativistic particles. The same criteria have been applied to all four reactions. Several possible sources of contamination of the 4C sample have been studied and are described in ref. 1. On the basis of these studies, we conclude that the overall contamination of the 4C sample is smaller than 7%.

III. Cross Section

The cross sections which we obtained from these data, after correcting for scanning losses and for beam contamination, are:

$$\sigma(pp \to pp\,\pi^+\pi^-) = (0.72 \pm 0.04)\ \text{mb} \quad (5)$$

$$\sigma(K^+p \to K^+p\,\pi^+\pi^-) = (0.38 \pm 0.07)\ \text{mb} \quad (6)$$

$$\sigma(\pi^+p \to \pi^+p\,\pi^+\pi^-) = (0.68 \pm 0.03)\ \text{mb} \quad (7)$$

$$\sigma(\pi^-p \to \pi^-p\,\pi^+\pi^-) = (0.67 \pm 0.04)\ \text{mb} \quad (8).$$

The value quoted in (6) extends the measurement of the cross section of reaction (2) from 32 GeV/c to 147 GeV/c. For reaction (3), we extend the information from 23 GeV/c to 147 GeV/c. For reactions (1) and (4), cross section measurements exist up to 205 GeV/c. We thus are able to perform an energy dependence study of the cross section for reactions (1)- (4) over a significant region of incident energy.

Figures 2(a) - 2(d) show the cross section of reactions (1) - (4), respectively, as a function of the incident beam momentum. In addition to the 147 GeV/c points from the present experiment, we have plotted published data above 5 GeV/c. For reaction (1), we have used data up to 205 GeV/c [7]; for reaction (2), the published data went up to 32 GeV/c [8]; for reaction (3) we used published data up to 23 GeV/c [9]; and for reaction (4) - data up to 205 GeV/c [1, 2, 10].

All figures show a similar trend of a decreasing cross section with increasing momentum. We have fitted the data of each of the four reactions (1) - (4) to the form

$$\sigma = A + B\ p^{-n} \quad (9)$$

where p is the incident beam laboratory momentum and A, B, n are constants to be determined by the fit. The results obtained from this fit are the following:

$$\sigma\,(pp \to pp\,\pi^+\pi^-) = (0.48 \pm 0.10) + (7.4 \pm 0.7)\,p^{(-0.6 \pm 0.1)} \quad (10)$$

$$\sigma\,(K^+p \to K^+p\,\pi^+\pi^-) = (0.34 \pm 0.08) + (7.3 \pm 1.5)\,p^{(-1.0 \pm 0.1)} \quad (11)$$

$$\sigma\,(\pi^+p \to \pi^+p\,\pi^+\pi^-) = (0.63 \pm 0.04) + (14.5 \pm 1.3)\,p^{(-1.2 \pm 0.1)} \quad (12)$$

$$\sigma\,(\pi^-p \to \pi^-p\,\pi^+\pi^-) = (0.62 \pm 0.04) + (3.7 \pm 1.4)\,p^{(-0.9 \pm 0.2)} \quad (13)$$

The value of n is about 1 for the incident meson beams and 0.6 for the p beam. The asymptotic values of the cross section for the π^+ and π^- beam reactions (3) and (4), respectively, are the same, as expected. They are higher than those of reactions (1) and (2).

The decrease of the cross section with momentum is presumably associated with the two-body meson exchange channels in the reactions (1) - (4), e.g.,

$$pp \to \Delta^{++}\,\Delta^0 \quad (14)$$

$$K^+p \to \Delta^{++}\,K^{*0} \quad (15)$$

$$\pi^+p \to \Delta^{++}\,\rho^0 \quad (16)$$

$$\pi^-p \to \Delta^0\,\rho^0 \quad (17).$$

Reactions (16) and (17) are restricted to odd G-parity exchange, while no such restriction applies to that of reaction (14). This may account for the difference between the meson and baryon induced reaction with respect to the value of n appearing in expression (9). In the case of reaction (15), although both even and odd G-parity exchanges are allowed, π-exchange has been shown to dominate that reaction [8].

For completeness we conclude this section with six-prong, 4-constraint cross section values for the following reactions: $\sigma\,(pp \to pp\pi^+\pi^+\pi^-\pi^-) = (0.260 \pm 0.040)$mb, $\sigma\,(\pi^+p \to \pi^+p\pi^+\pi^+\pi^-\pi^-) = (0.205 \pm 0.025)$mb, and $\sigma\,(\pi^-p \to \pi^-p\pi^+\pi^+\pi^-\pi^-) = (0.185 \pm 0.025)$mb.

IV. Single Diffraction

In this section we discuss that part of the cross section coming either from the diffraction of the incident beam or that of the target proton. In order to do so, we define all events with Feynman x of the outgoing proton less than -0.96 to be beam diffraction events. All events with x of the fastest outgoing particle (leading particle) greater than 0.96 are defined as proton diffraction.

With these definitions, we obtain the following results:

$$\sigma(pp \to p^*_{beam} p) = (0.29 \pm 0.03) \text{ mb}$$
$$\sigma(pp \to pp^*_{target}) = (0.34 \pm 0.03) \text{ mb} \quad (18)$$

$$\sigma(K^+ p \to K^* p) = (0.20 \pm 0.04) \text{ mb}$$
$$\sigma(K^+ p \to K^+ p^*) = (0.13 \pm 0.04) \text{ mb} \quad (19)$$

$$\sigma(\pi^+ p \to \pi^* p) = (0.37 \pm 0.02) \text{ mb}$$
$$\sigma(\pi^+ p \to \pi^+ p^*) = (0.23 \pm 0.02) \text{ mb} \quad (20)$$

$$\sigma(\pi^- p \to \pi^* p) = (0.35 \pm 0.03) \text{ mb}$$
$$\sigma(\pi^- p \to \pi^- p^*) = (0.23 \pm 0.02) \text{ mb} \quad (21)$$

For all four reactions, (1) - (4), the sum of the beam and target diffraction cross sections accounts for about 90% of the total channel cross section. This is expected at high energies and also explains the almost equal cross sections (7) and (8).

Let us define R_a as the ratio of beam to target diffraction cross section for beam particle a:

$$R_a = \frac{\sigma(a\,p \to a^* p)}{\sigma(a\,p \to a\,p^*)} . \quad (22)$$

With this definition, we find $R_p = 0.9 \pm 0.1$, $R_{K^+} = 1.5 \pm 0.5$, $R_{\pi^+} = 1.6 \pm 0.2$,

and $R_{\pi^-} = 1.5 \pm 0.2$. The value of R_p is in agreement with the expected value of 1 for the symmetric pp reaction. That the value of the ratio (22) is larger than 1 for the other beams reflects the fact that the Pomeron-p-p coupling is larger than the Pomeron-meson-meson coupling.

V. Double Pomeron

The DPE reactions are difficult to study. There does not exist a precise definition of a DPE sample and usually there are difficulties arising from lack of statistical resolution.

One definition of the DPE region is given [11] by a cut on the variable

$$Z_i = \ell n\,(s/M_{xi}) \simeq \ell n\,\left(\frac{1}{1-|x_i|}\right) \qquad (23)$$

where s is the square of the total center-of-mass energy, M^2_{xi} is the invariant mass squared recoiling against particle i, and x_i is the Feynman variable - $x = \frac{2P_L}{\sqrt{s}}$ for particle i. The DPE region is defined as that which satisfies both $Z_a \cdot Z_p \geq \ell n\ 10 = 2.3$. In addition, for either of these definitions the rapidity of each of the central pions in the overall center-of-mass, Y^*_π, must be near zero to ensure a large rapidity gap between the central and the leading particles.

Figures 3(a) - 3(d) show the triangle plot of Z_a versus Z_p for the reactions (1) - (4), respectively. The two variables Z_a and Z_p span a triangular region of phase space which is limited by

$$(Z_a + Z_p) < \ell n\,(s/s_0)$$

where $s_0 = 0.14\ \mathrm{GeV}^2$. The lines correspond to the values $Z_a = Z_p = 2.3$. As can be seen, most events lie in the region where either Z_a or Z_p is large, but not both. These are the single diffractive events described by Figs. 1(a) and 1(b). The events in the region where Z_a and Z_p are both larger than 2.3 have been defined

as possible DPE events [11]. Table I gives the number of events and the corresponding cross sections. Reaction (2) has no events in this region, and we can therefore only give an upper limit to the cross section for DPE production in this reaction.

The properties expected in DPE events can be summarized as follows [3]: (a) both leading particles should have nearly the full longitudinal momentum, $|x| \approx 1$; (b) the sum of the rapidities of the remaining two pions should be small; (c) the invariant mass of combinations containing one of the leading particles is expected to be large; and (d) the invariant mass of the remaining di-pion system should not show a $\rho(765)$ signal. This last is the consequence of the fact that if only DPE is present, the allowed quantum numbers of the $\pi^+\pi^-$ system are restricted to $I = 0$ and $J^P = 0^+, 2^+, 4^+ \ldots$

We studied these features in all events of reactions (1), (3), and (4) which satisfied the conditions $Z_a > 2.3$ and $Z_p > 2.3$. These cuts ensure that $|x| > 0.9$ for particle a and the proton p. Figures 4(a) to 4(d) show the sum of the center-of-mass rapidities of the π^+ (the slower one in reaction (3)) and the π^- (the slower one in reaction (4)) for all events in reactions (1) - (4). One clearly observes two peaks centered around ± 4.5 which correspond to the single diffractive dissociation described by the diagram in Figs. 1(a) and 1(b). In the central region, the shaded events are those satisfying the DPE criteria of ref. 11. As mentioned above, no such events are found for reaction (2), where our number of events is very low.

Figure 5 shows the invariant mass distributions of all di-pion systems. A clear ρ (765) signal is observed in reactions (3) and (4) . There is a suggestion

of ρ in the other two reactions as well. The strongest source of p's in reactions (3) and (4) is the decay into $\rho^0\pi$ of the $(\pi^{\pm}\pi^+\pi^-)$ system produced via single Pomeron exchange, as will be discussed in the next section. Neither of the diffractively produced $(p\pi^+\pi^-)$ or $(K^+\pi^+\pi^-)$ systems has a strong decay mode into $p\rho^0$ or $K^+\rho^0$, and therefore very little ρ^0 signal is observed in reactions (1) and (2). The shaded area is the invariant mass distribution of $\pi^+\pi^-$ coming from the DPE events. These distributions show no ρ signal.

We have also checked the invariant masses of combinations involving one of the leading particles, such as $(p\pi^+)$ or $(p\pi^+\pi^-)$. Although a strong Δ^{++} signal is seen in all four reactions, coming mainly from the decay of the diffractively produced $(p\pi^+\pi^-)$ system, the DPE sample has no events in either the Δ^{++} region or in the low-mass $(p\,\pi^+\pi^-)$ region. No other mass combinations show any low-mass concentration. Column 4 of Table I presents the double Pomeron cross sections for reactions (1) - (4) based on the shaded DPE candidates of Fig. 4. Insofar as those candidates are compatible with the tails of the single diffraction distributions, our DPE cross sections are effectively upper limits.

The DPE cross sections for different reactions at a given energy are related to each other as follows [12]:

$$\sigma_{DPE}\ (pp) \simeq 2\sigma_{DPE}\ (\pi p) \simeq 4\sigma_{DPE}\ (Kp)\ . \qquad (24)$$

Since we have measured all these interactions at the same energy with the same apparatus and have analyzed them using the same procedure, systematic differences are minimized and we can perform a good test of relation (24). Figure 6(a) shows our measured cross sections at 147 GeV/c for the four reactions (1) - (4), together with the theoretical predictions [12]. As can be seen in Fig. 6(a), the predictions of relation (24) are indeed borne out by the data. In the same figure, we have also

included for comparison, data at 205 GeV/c as analyzed in ref. 11, using the same definition of DPE as in our experiment. These data points agree well with our measurements.

Figure 6(b) shows the energy dependence of the DPE cross sections for reaction (1) using our result and those of ISR experiments [3]. Since the latter were obtained using cuts ($|Y^*_\pi| < 1$ and $|Y^*_\pi| < 1.5$) on the rapidity of the pions, we have made the same cuts on our data. The values which we obtain are given in the last column of Table I. The dotted lines in Fig. 6(b) are the corresponding theoretical predictions of ref. 13. Although not all the data are in good agreement with the predictions, their general trend follows the theoretical expectations.

VI. $\pi^\pm$ beam diffraction

Figure 7(a) shows the $\pi^+\pi^-\pi^-$ mass distribution of reaction (3) and Fig. 7(b) shows the $\pi^+\pi^+\pi^-$ mass distribution of reaction (4). The two mass distributions look very similar and show a low-mass enhancement in the A_1-A_2 mass region. Both figures show a strong ρ^0 decay mode, as can be seen from the shaded part of the histograms. Figure 7(c) shows the combined $\rho^0\pi^\pm$ mass distribution of reactions (3) and (4). We define the ρ^0 as the $\pi^+\pi^-$ combinations lying between the mass values 0.66 - 0.86 GeV.

Figure 8 shows a compilation of cross section values for the production of 3π with masses $1.2 < M_{3\pi} < 1.4$ GeV in reactions (3) and (4), with incident beam momentum $p_{lab} > 10$ GeV/c. Data for reaction (3) are taken from ref. 14, while data for reaction (4) have been calculated from information in ref. 15. The straight line is the result of a fit to the data, of the form

$$\sigma = A\, p_{lab}^{-n} \qquad (25)$$

with a slope of $n = 0.23 \pm 0.05$. An energy behavior with such a small slope

indicates diffractive production. The value of n is close to the value of 0.25 ± 0.01 found for elastic scattering between 7 and 40 GeV/c [16].

In addition to a weak energy dependence of the cross section, diffraction processes are characterized among others by: (a) equality of particle and anti-particle cross sections on the same target, and (b) sharp forward peak in the differential cross section. As seen from Fig. 8, the cross section for the mass interval 1.2 - 1.4 GeV produced in reaction (3) at 147 GeV/c, (0.084 ± 0.013)mb, is very close to that produced in reaction (4) at the same energy, (0.080 ± 0.011)mb. In Fig. 9, we show the differential cross section $d\sigma/dt'$ for the interval $1.2 < M_{3\pi} < 1.4$ GeV for reactions (3) and (4). $t' = |t - t_{min}|$, where t is the square of the four-momentum transfer between the target and the outgoing proton. A fit of the form

$$\frac{d\sigma}{dt'} = Ae^{-bt'} \tag{26}$$

to the data yields a slope of (8.6 ± 1.6) $(GeV/c)^{-2}$ for reaction (3) and (6.1 ± 1.0) $(GeV/c)^{-2}$ for reaction (4). These slopes are in good agreement with known diffractive processes like $\gamma \to \rho$ (6-8 $(GeV/c)^{-2}$) or elastic scattering (7-9 $(GeV/c)^{-2}$). Although the data have large error bars, one may even see a hint of the crossover phenomena with the crossing at $t' \sim 0.2$ $(GeV/c)^2$ - as expected from processes dominated by Pomeron exchange [17]. A similar crossover effect has been reported at 16 GeV/c [18] for the same final state.

From all these observations we are led to believe that the 3π mass interval 1.2 - 1.4 GeV is diffractively produced. This mass interval, which is usually associated with the A_2 region, is believed to have $J^P = 2^+$ quantum numbers. Diffractive production of a system with these quantum numbers from a $J^P = 0^-$ beam would be in violation of the Gribov-Morrison rule [19]. This rule states that the diffractively

produced systems should obey the relation

$$\Delta P = (-1)^{\Delta J} \qquad (27)$$

where ΔP and ΔJ are the changes in parity and angular momentum between the projectile and the diffractive system. From the very beginning it was noted, however, that A_2 production appears to violate this rule at lower energies [19]. This violation seems to persist up to an incident energy of 147 GeV/c for both negative and positive pion beams.

VII. Summary

We have measured the four prong-4C reaction at 147 GeV/c in pp, K^+p, π^+p, and π^-p interactions. All four reactions were measured with the same apparatus and analyzed in the same way.

We have studied the energy dependence of all four prong-4C production cross sections and found that they are consistent with $Ap^{-0.6} + B$ for the first reaction (reaction (1)) and $Ap^{-1} + B$ for the last three reactions (reactions (2), (3), and (4)). This difference in the energy dependence of the cross section could come from G-parity restrictions on the exchanged particle in the last two reactions. In addition, the K^+p reactions, though not restricted by G-parity, has been shown to be dominated by π-exchange [8].

We have found that about 90% of the total channel cross section at 147 GeV/c can be accounted for by either beam or target diffraction. The ratio of beam to target diffraction cross section is about 1 for the pp reaction and about 1.5 for the other three reactions. Some of the remaining cross sections may come from interactions mediated by double Pomeron exchange. We have isolated events satisfying DPE criteria and showed them to be consistent with predictions of a DPE model [12].

We have studied the $\pi^\pm$ beam diffraction into a low-mass 3π enhancement in the A_1 - A_2 mass region. The 3π in the mass region 1.2 - 1.4 GeV is shown to be diffractively produced, and if this region is assumed to be dominated by A_2 ($J^P = 2^+$) production, this observation would violate the Gribov-Morrison rule [19].

Acknowledgment

This work was supported in part by the U. S. Department of Energy, the National Science Foundation, the Israeli Academy of Science (Commission for Basic Research), the U. S. -Israel Binational Science Foundation, and the Dutch Foundation for Fundamental Research of Energy. We gratefully acknowledge the efforts of the 30-inch bubble chamber crew and the scanning and measuring personnel at the participating institutions.

Footnotes and References

(a) Now at the University of Liverpool, Liverpool, England.

(b) Now at Université de Neuchâtel, Neuchâtel, Switzerland.

(c) Now at Duke University, Durham, North Carolina 27706, USA.

(d) On leave of absence from University of Pavia, Pavia, Italy.

(e) On leave of absence from Institute of High Energy Physics, Beijing, PRC.

(f) On leave of absence from Collège de France, Paris, France.

(g) On leave of absence from Nara Women's University, Nara, Japan.

(h) Present address: Automatix, Burlington, Massachusetts 01803, USA.

(i) Now at Maritiem Research Instituut Nederland, Wageningen, The Netherlands.

(j) Now at CERN, Geneva, Switzerland.

(k) Permanent address: Set Hall University, South Orange, New Jersey 07079, USA.

(l) Now at Brookhaven National Laboratory, Upton, New York 11973, USA.

1. D. Fong et al., Nuovo Cimento 34A, 659 (1976).

2. H. H. Bingham et al., Phys. Lett. 51B, 397 (1974).

3. M. Derrick, B. Musgrave, P. Schreiner, H. Yuta, Phys. Rev. Lett. 32, 80 (1974); D. Denegri et al., Nucl. Phys. B98, 189 (1975); L. Baksay et al., Phys. Lett. 61B, 89 (1976); M. Della Negra et al., Phys. Lett. 65B, 394 (1976); D. Drijard et al., Nucl. Phys. B143, 61 (1978); H. De Kerret et al., Phys. Lett. 68B, 385 (1977).

4. S. Nussinov, private communication.

5. D. Fong et al., Phys. Lett. 53B, 290 (1974); Phys. Lett. 60B, 124 (1975); Nucl. Phys. B102, 386 (1976); Phys. Lett. 61B, 99 (1976); Nucl. Phys. B104, 32 (1976); Phys. Rev. Lett. 37, 736 (1976); D. Brick et al., Phys. Rev. D18, 3099 (1978); F. Barreiro et al., Nucl. Phys. B148, 41 (1979); D. Brick et al., Phys. Rev. D19, 743 (1979); Nucl. Phys. B150, 109 (1979); Phys. Rev. D21, 1726 (1980).

References (contd.)

6. D. Brick et al., Phys. Rev. D21, 632 (1980); Nucl. Phys. B164, 1 (1980); M. Schouten et al., Z. Phys. C9, 93 (1981).

7. E. Gellert et al., Phys. Rev. Lett. 17, 884 (1966); G. Alexander et al., Phys. Rev. 154, 1284 (1967); A. P. Colleraine and U. Nauenberg, Phys. Rev. 161, 1387 (1967); W. Chinowsky et al., Phys. Rev. 171, 1421 (1968); S. P. Almeida, J. G. Rushbrooke, J. H. Scharenguivel, Phys. Rev. 174, 1638 (1968); R. Ehrlich et al., Phys. Rev. Lett. 21, 1839 (1968); C. Caso, F. Conte, G. Tomasini, Nuovo Cimento 55A, 66 (1968); G. Kayas et al., Nucl. Phys. B5, 169 (1968); G. Yekutieli et al., Nucl. Phys. B18, 301 (1970); E. Colton, P. E. Schlein, E. Gellert, G. A. Smith, Phys. Rev. D3, 1063 (1971); J. G. Rushbrooke et al., Phys. Rev. D4, 3273 (1971); H. Boggild et al., Nucl. Phys. B27, 285 (1971); J. Le Guyader et al., Nucl. Phys. B35, 573 (1971); W. Burdett et al., Nucl. Phys. B48, 13 (1972); M. Derrick, B. Musgrave, P. Schreiner, H. Yuta, Phys. Rev. D9, 1215 (1974); K. von Holt et al., Nucl. Phys. B103, 221 (1976).

8. F. Bomse et al., Phys. Rev. Lett. 20, 1519 (1968); D. C. Colley et al., Nucl. Phys. B26, 71 (1971); R. Mercer et al., Nucl. Phys. B32, 381 (1971); E. de Wolf, Y. Goldschmidt-Clermont, F. Grard, F. Verbeure, Nucl. Phys. B46, 333 (1972); H. H. Bingham et al., Nucl. Phys. B48, 589 (1972); D. C. Colley et al., Nucl. Phys. B55, 1 (1973); G. Ciapetti et al., Nucl. Phys. B64, 58 (1973); A. Stergiou et al., Nucl. Phys. B102, 1 (1976); A. Givernaud et al., Nucl. Phys. B153, 280 (1979).

9. P. Slattery, H. Kraybill, B. Forman, T. Ferbel, Nuovo Cimento 50A, 377 (1967); J. A. Gaidos et al., Phys. Rev. D1, 3190 (1970); C. L. Pols et al., Nucl. Phys. B25, 109 (1971); I. J. Bloodworth, W. C. Jackson, J. D. Prentice, T. S. Yoon, Nucl. Phys. B35, 79 (1971); C. Caso et al., Nucl. Phys. B36, 349 (1972);

S. Lichtman et al., Nucl. Phys. B81, 31 (1974); P. Bosetti et al., Nucl. Phys. B101, 304 (1975); J. Bartke et al., Nucl. Phys. B120, 1 (1977); C. Baltay et al., Phys. Rev. D17, 62 (1978).

10. N. N. Biswas, I. Derado, N. Schmitz, W. D. Shephard, Phys. Rev. 134B, 901 (1964); N. M. Cason, Phys. Rev. 148, 1282 (1966); S. Miyashita, J. von Krogh, J. B. Kopelman, L. M. Libby, Phys. Rev. D1, 771 (1970); A. R. Dzierba et al., Phys. Rev. D2, 2544 (1970); G. W. Brandenburg et al., Nucl. Phys. B16, 287 (1970); J. Ballam et al., Phys. Rev. D4, 1946 (1971); K. F. Galloway et al., Phys. Rev. D5, 1097 (1972); N. Armenise et al., Nuovo Cimento Lett. 4, 201 (1972); P. P. Antich, G. Cecchet, S. Ratti, R. Rivosecchi, Nuovo Cimento Lett. 5, 941 (1972); A. D. Johnson et al., Phys. Rev. D7, 1314 (1973); S. Lichtman et al., Nucl. Phys. B81, 31 (1974); J. Brau et al., Nucl. Phys. B99, 282 (1975).

11. D. M. Chew, Nucl. Phys. B82, 422 (1974).

12. D. M. Chew and G. F. Chew, Phys. Lett. 53B, 191 (1974).

13. D. M. Chew, Phys. Lett. 65B, 367 (1976).

14. Yu. M. Antipov et al., Nucl. Phys. B63, 141 (1973); B63, 153 (1973); U. E. Kruse et al., Phys. Rev. Lett. 32, 1328 (1974); K. Paler, Nucl. Phys. B18, 211 (1970); G. Ascoli et al., Phys. Rev. D7, 669 (1973).

15. C. Caso et al., Nucl. Phys. B36, 349 (1972); S. Lichtman et al., Nucl. Phys. B81, 31 (1974); C. Baltay et al., Phys. Rev. D17, 62 (1978).

16. Yu. M. Antipov et al., Nucl. Phys. B57, 333 (1973).

17. V. D. Barger and D. B. Cline, Phenomenological Theories of High Energy Scattering, New York, W. E. Benjamin (1969).

18. J. V. Beaupré et al., Phys. Lett. 41B, 393 (1972).

19. V. N. Gribov, Yad. Fiz. (USSR) 5, 197 (1967); D. R. O. Morrison, Phys. Rev. 165, 1699 (1968).

Table Caption

Table I Channel and double Pomeron cross section for reactions (1) - (4)

TABLE I

Channel	σ(mb)	N_{DPE}	σ_{DPE}(μb)	$\lvert Y_\pi \rvert < 1.0$	$\lvert Y_\pi \rvert < 1.5$
$pp \to pp\pi^+\pi^-$	.72 ± .04	18.5	49 ± 11	30 ± 9μb	46 ± 11μb
$K^+p \to K^+p\pi^+\pi^-$	.38 ± .07	0	< 11		
$\pi^+p \to \pi^+p\pi^+\pi^-$	.68 ± .03	14	22 ± 6		
$\pi^-p \to \pi^-p\pi^+\pi^-$	.67 ± .04	15	29 ± 8		

Figure Captions

Fig. 1 Diagrams representing (a) single diffraction of the target, (b) single diffraction of the beam, (c) associated resonance production, (d) two-particle exchange with resonance production at the target vertex, (e) two-particle exchange with resonance production at the beam vertex, and (f) double Pomeron exchange.

Fig. 2 Variation of the cross section σ as a function of laboratory momentum p for the reactions (a) $pp \to pp\,\pi^+\pi^-$, (b) $K^+p \to K^+p\,\pi^+\pi^-$, (c) $\pi^+p \to \pi^+p\,\pi^+\pi^-$, and (d) $\pi^-p \to \pi^-p\,\pi^+\pi^-$.

Fig. 3 The triangle plot of Z_a versus Z_p for events of the reactions (a) $pp \to pp\pi^+\pi^-$, (b) $K^+p \to K^+p\pi^+\pi^-$, (c) $\pi^+p \to \pi^+p\,\pi^+\pi^-$, and (d) $\pi^-p \to \pi^-p\,\pi^+\pi^-$.

Fig. 4 Sum of the center-of-mass rapidities of the π^+ and π^- produced in the reactions (a) $pp \to pp\,\pi^+\pi^-$, (b) $K^+p \to K^+p\,\pi^+\pi^-$, (c) $\pi^+p \to \pi^+p\,\pi^+\pi^-$ (the slower π^+ for this reaction) and (d) $\pi^-p \to \pi^-p\,\pi^+\pi^-$ (the slower π^- for this reaction). The shaded events are those satisfying the DPE criteria (see text).

Fig. 5 The $\pi^+\pi^-$ invariant mass distribution of the events of the reactions (a) $pp \to pp\,\pi^+\pi^-$, (b) $K^+p \to K^+p\,\pi^+\pi^-$, (c) $\pi^+p \to \pi^+p\,\pi^+\pi^-$, and (d) $\pi^-p \to \pi^-p\,\pi^+\pi^-$. The shaded events are those satisfying the DPE criteria (see text).

Fig. 6 (a) Double Pomeron cross section as a function of the lab momentum. The dotted lines are a prediction of a DPE calculation of ref. 12. The data at 205 GeV/c are taken from an analysis of ref. 8; ● - pp, x - π^+p, o - π^-p, and + - K^+p. (b) s-dependence of the double Pomeron cross section using data from this experiment (■) and from ISR experiments

Figure Captions (contd.)

Fig. 6 (●, ▲- ref. 3) for rapidity cut $|Y^*_\pi| < 1.0$. Also from this experiment (□) and from ISR experiments (o, △ - ref. 3) for rapidity cut $|Y^*_\pi| < 1.5$. The dotted lines are predictions of ref. 13.

Fig. 7 Mass of the 3π system. Events with either or both M ($\pi^+\pi^-$) between 0.66 and 0.86 GeV (ρ region) are shaded in (a) events belonging to reaction (3), (b) events from reaction (4), and (c) mass of the 3π system from reactions (3) and (4) with either or both M($\pi^+\pi^-$) in the ρ region.

Fig. 8 $\pi^\pm p \to \pi^\pm\pi^+\pi^- p$ cross section versus beam momentum for the 3π mass band of 1.2 - 1.4 GeV. The straight line is the best fit of the form $\sigma = Ap^{-n}$ to the data.

Fig. 9 Differential cross section $d\sigma/dt'$ as a function of t' for the 3π mass region 1.2 - 1.4 GeV with either or both M ($\pi^+\pi^-$) in the ρ region (0.66 - 0.86 GeV) for events from reaction (3) - (o) and those from reaction (4) - (●).

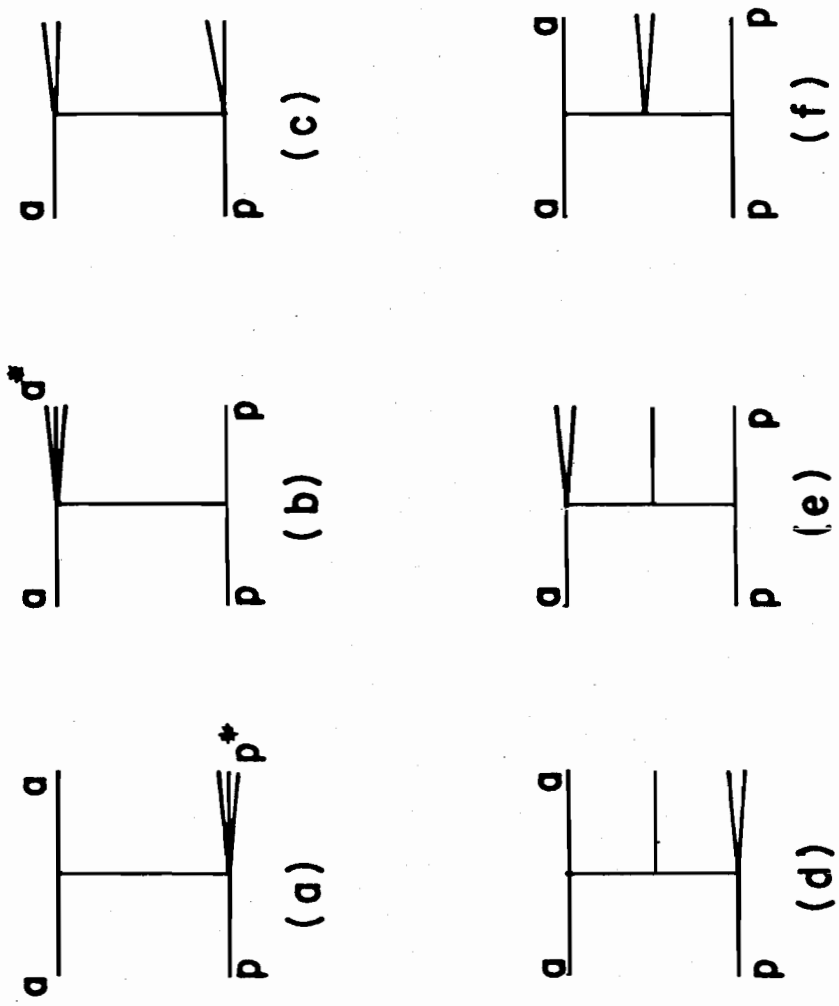

Figure 1

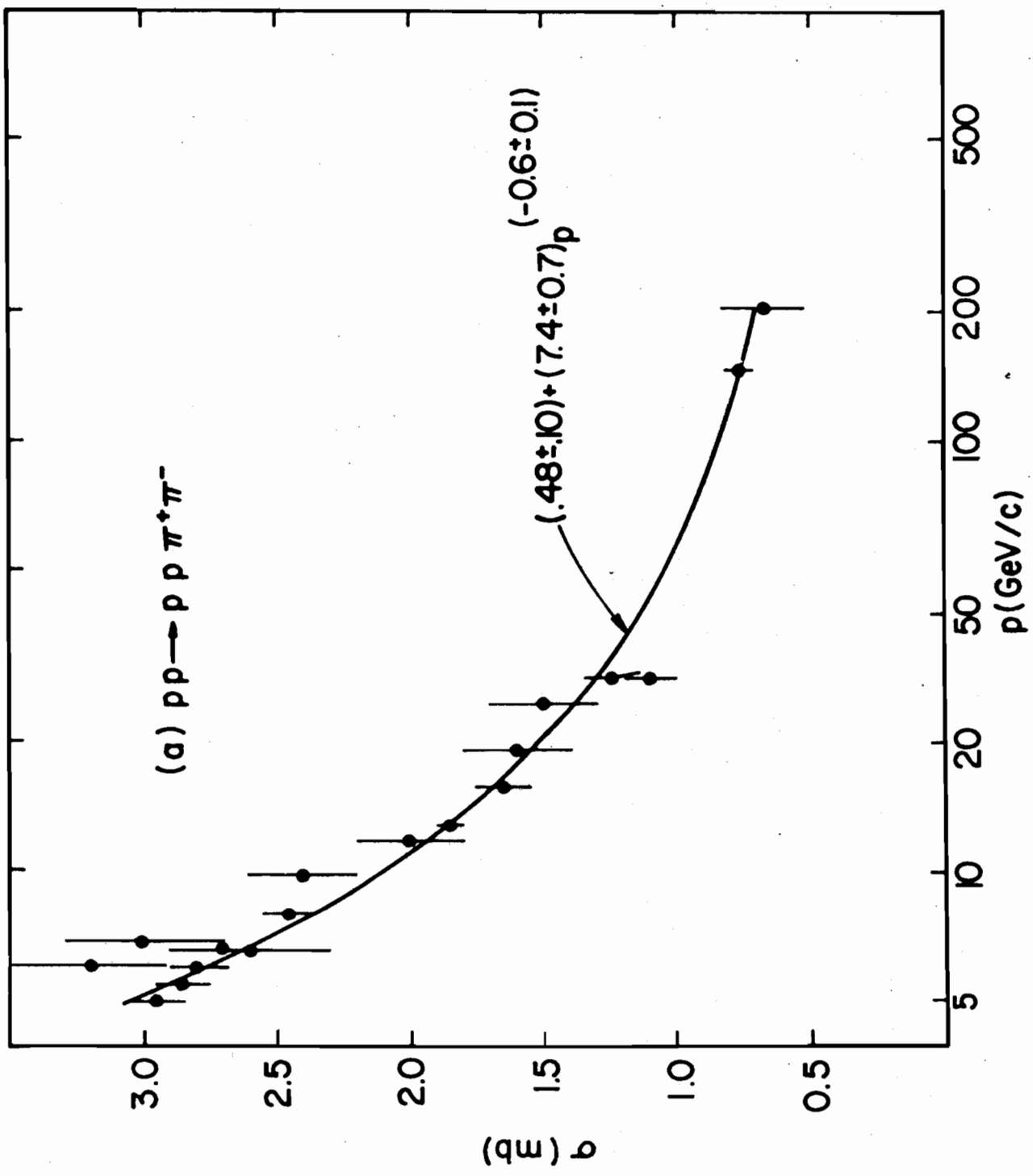
(a) pp → p p π⁺π⁻
(.48±.10)+(7.4±0.7)p^(-0.6±0.1)
σ (mb)
p(GeV/c)
3.0
2.5
2.0
1.5
1.0
0.5
5
10
20
50
100
200
500

Figure 2(a)

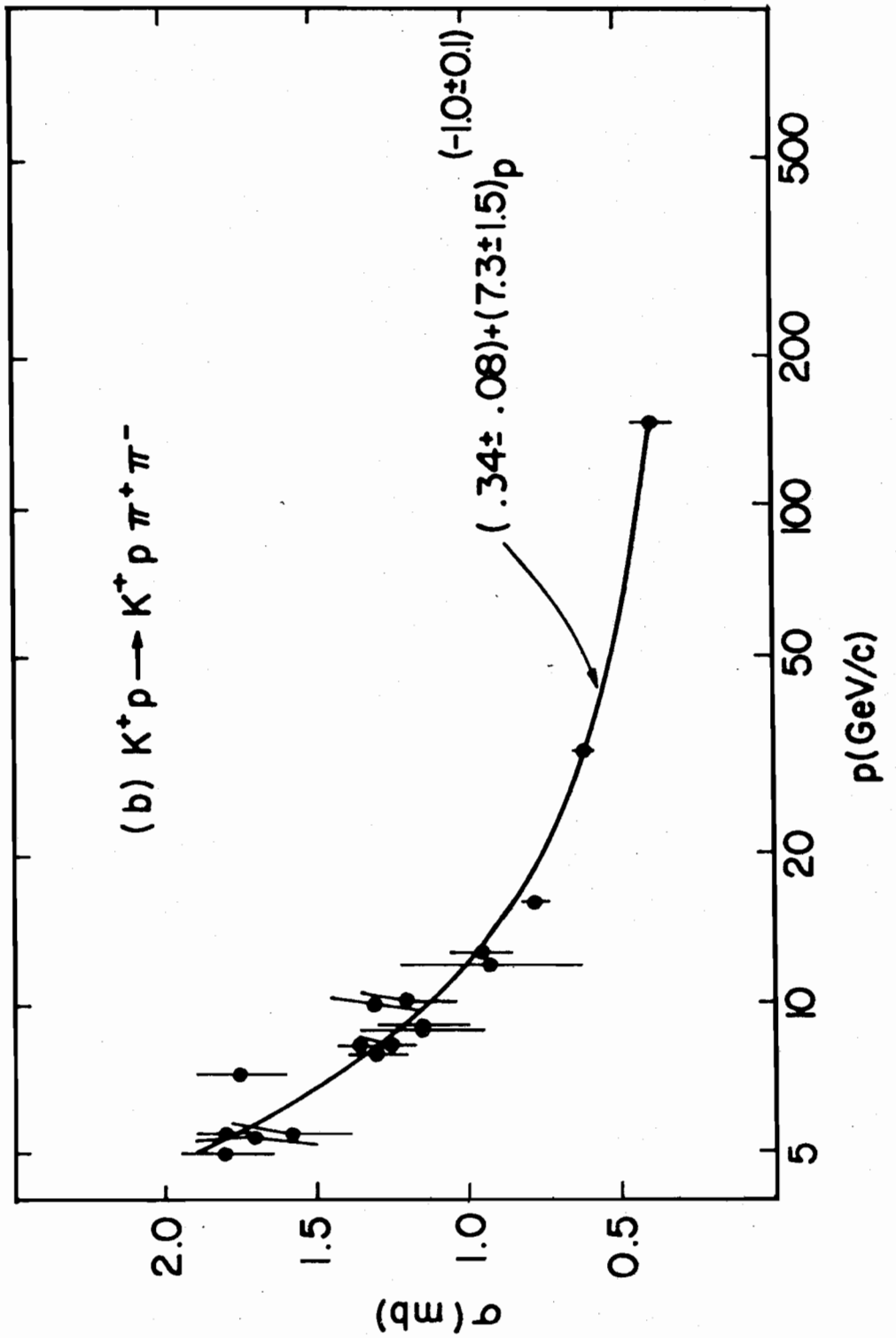
(b) $K^+p \rightarrow K^+p\pi^+\pi^-$
$(.34\pm .08)+(7.3\pm1.5)_p^{(-1.0\pm0.1)}$
σ (mb)
p(GeV/c)
2.0
1.5
1.0
0.5
5
10
20
50
100
200
500

Figure 2(b)

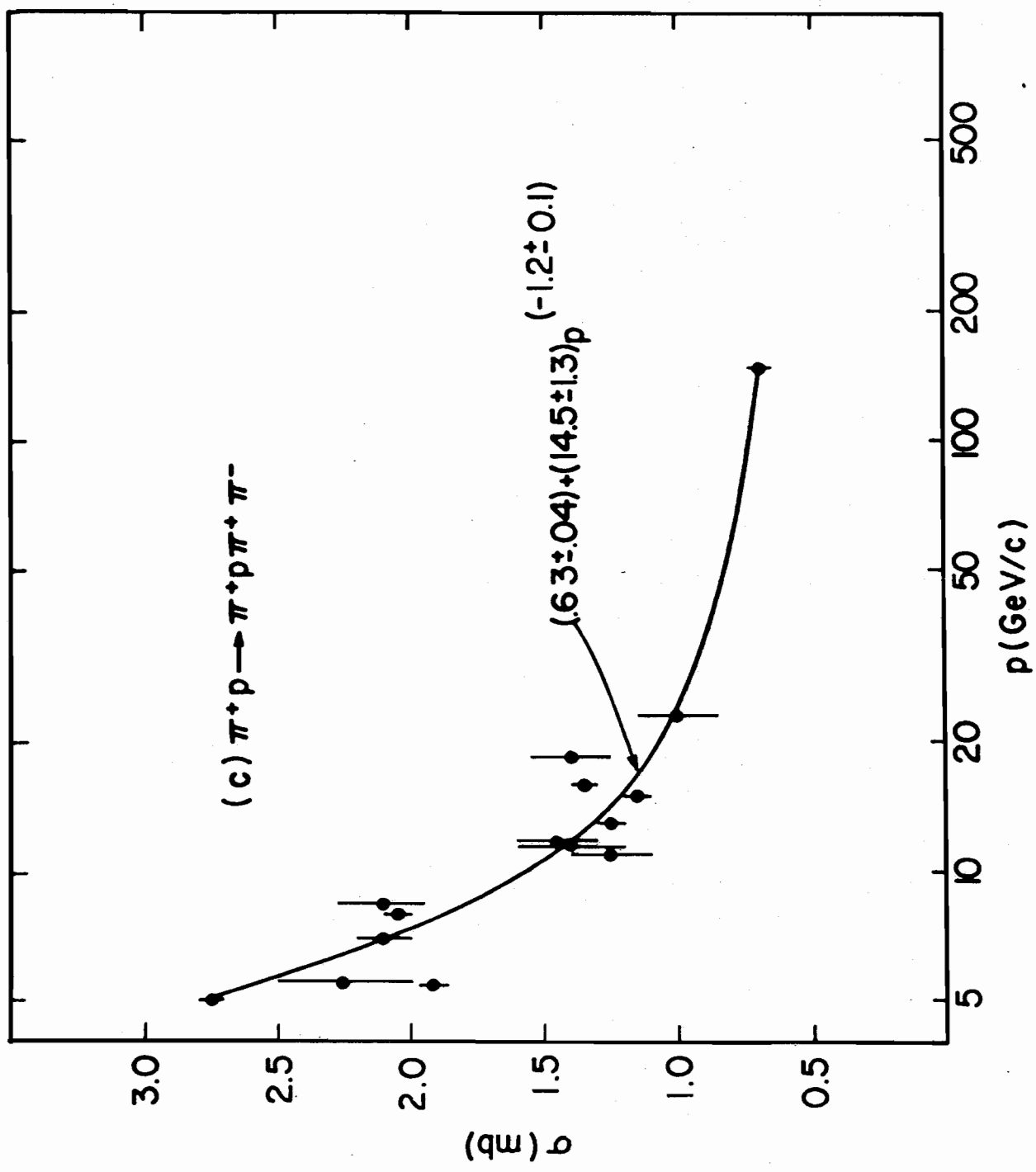
(c) $\pi^+ p \rightarrow \pi^+ p \pi^+ \pi^-$
$(.63 \pm .04) + (14.5 \pm 1.3) p^{(-1.2 \pm 0.1)}$
σ (mb)
p (GeV/c)
3.0
2.5
2.0
1.5
1.0
0.5
5
10
20
50
100
200
500

Figure 2(c)

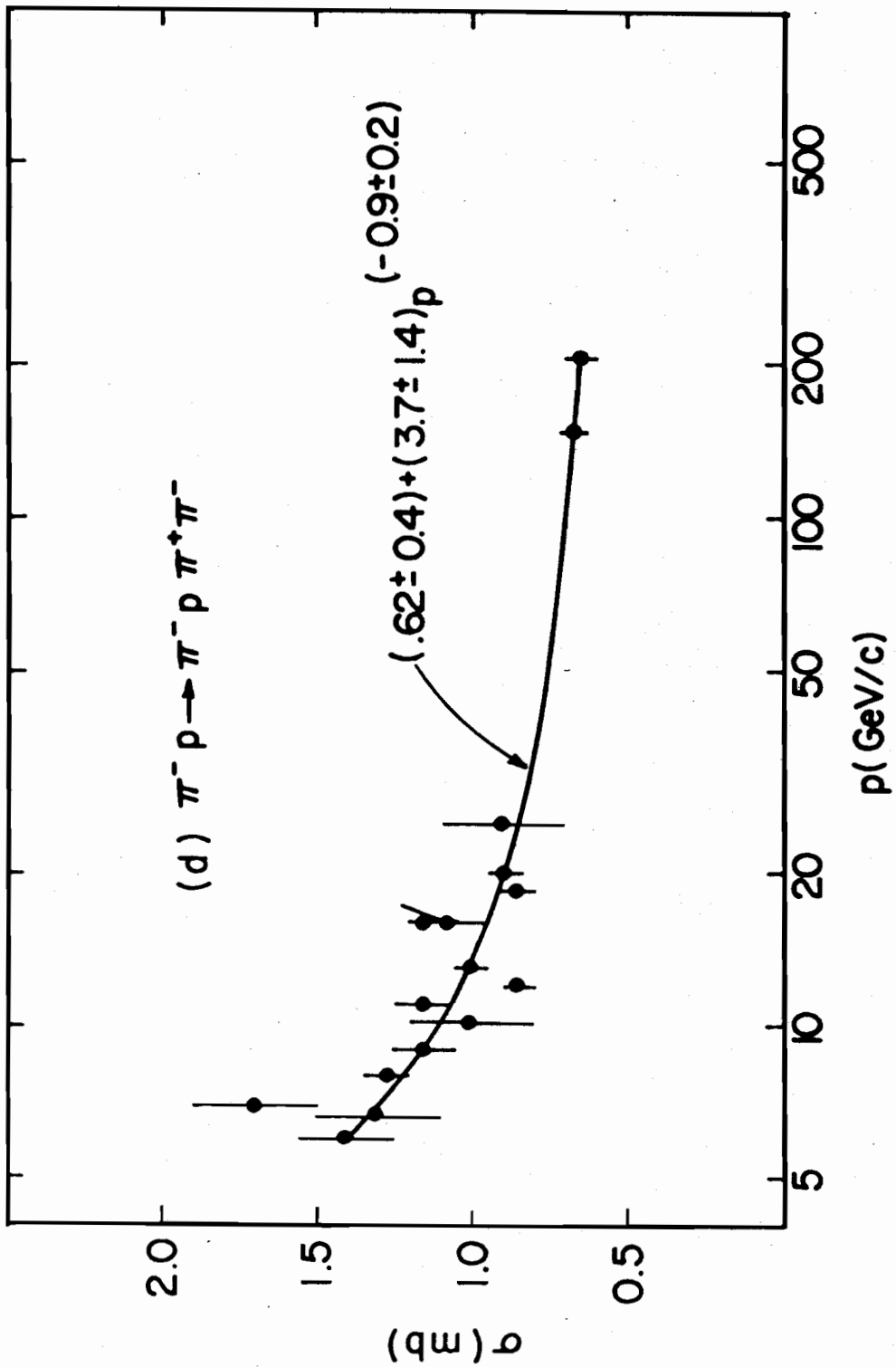
(d) $\pi^- p \to \pi^- p \pi^+ \pi^-$
$(.62 \pm 0.4) + (3.7 \pm 1.4)_p^{(-0.9 \pm 0.2)}$
σ (mb)
p(GeV/c)
2.0
1.5
1.0
0.5
5
10
20
50
100
200
500

Figure 2(d)

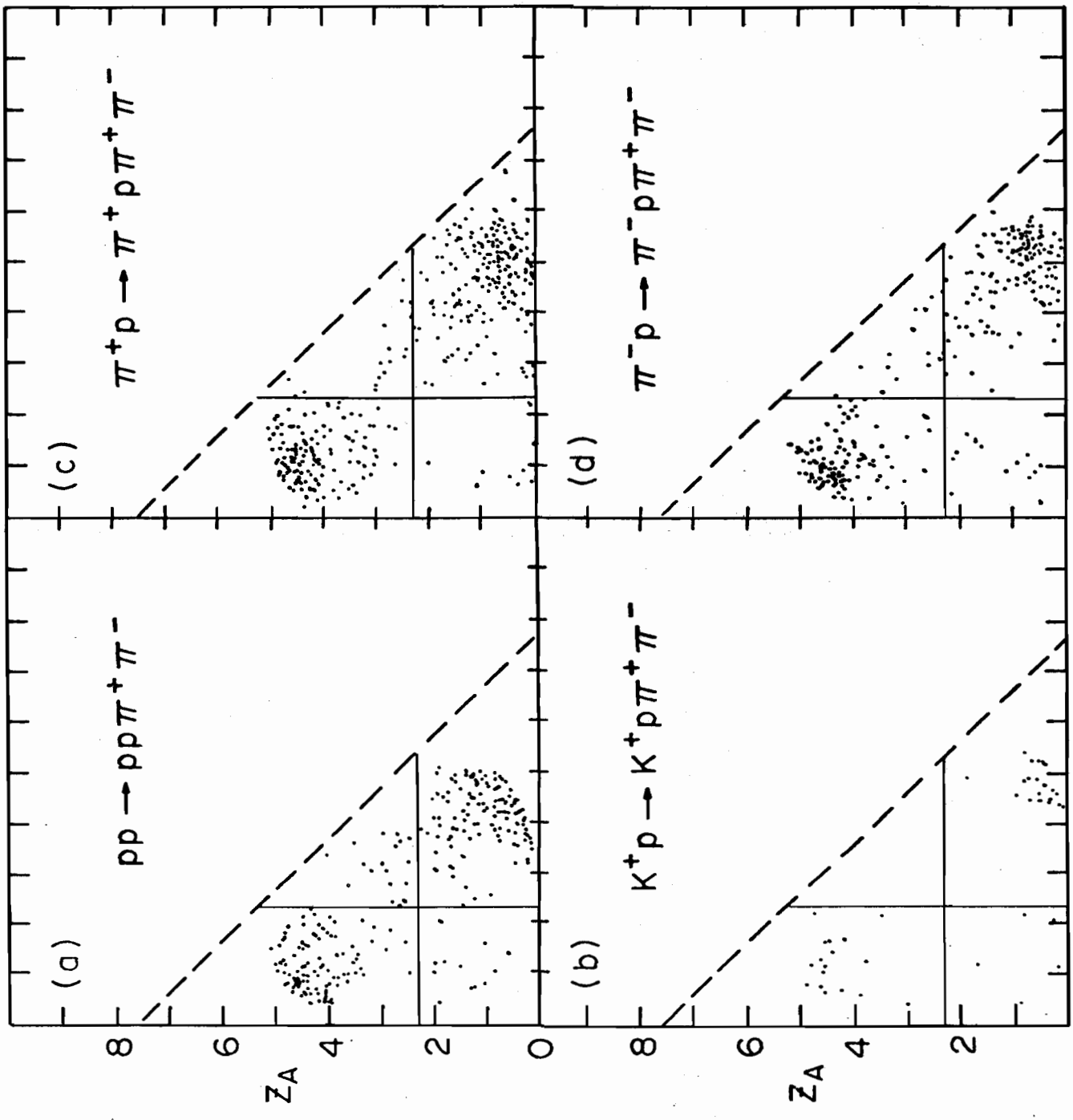

Figure 3

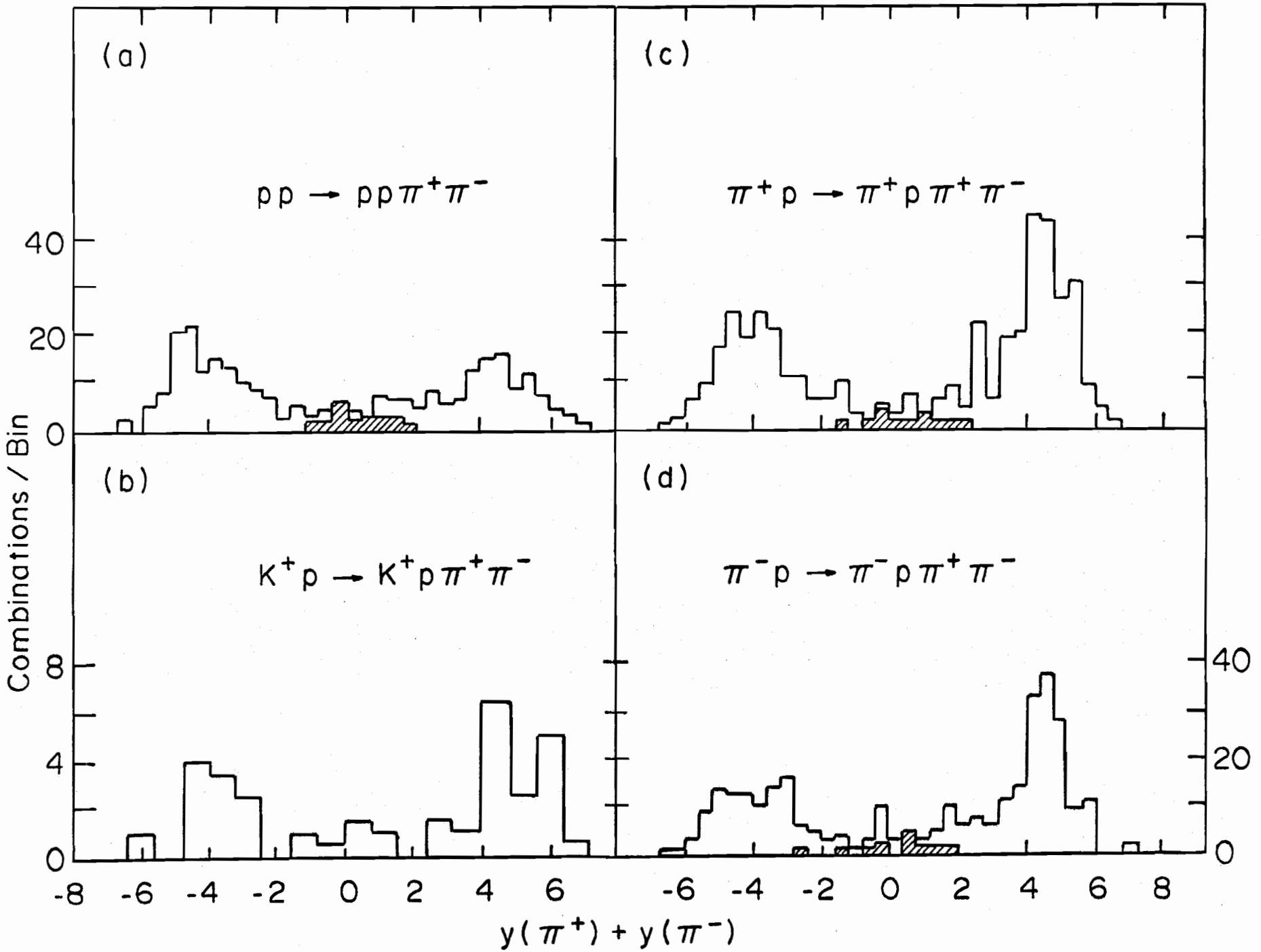
(a)
$pp \rightarrow pp\pi^+\pi^-$
(c)
$\pi^+p \rightarrow \pi^+p\pi^+\pi^-$
(b)
$K^+p \rightarrow K^+p\pi^+\pi^-$
(d)
$\pi^-p \rightarrow \pi^-p\pi^+\pi^-$
Combinations / Bin
$y(\pi^+) + y(\pi^-)$

Figure 4

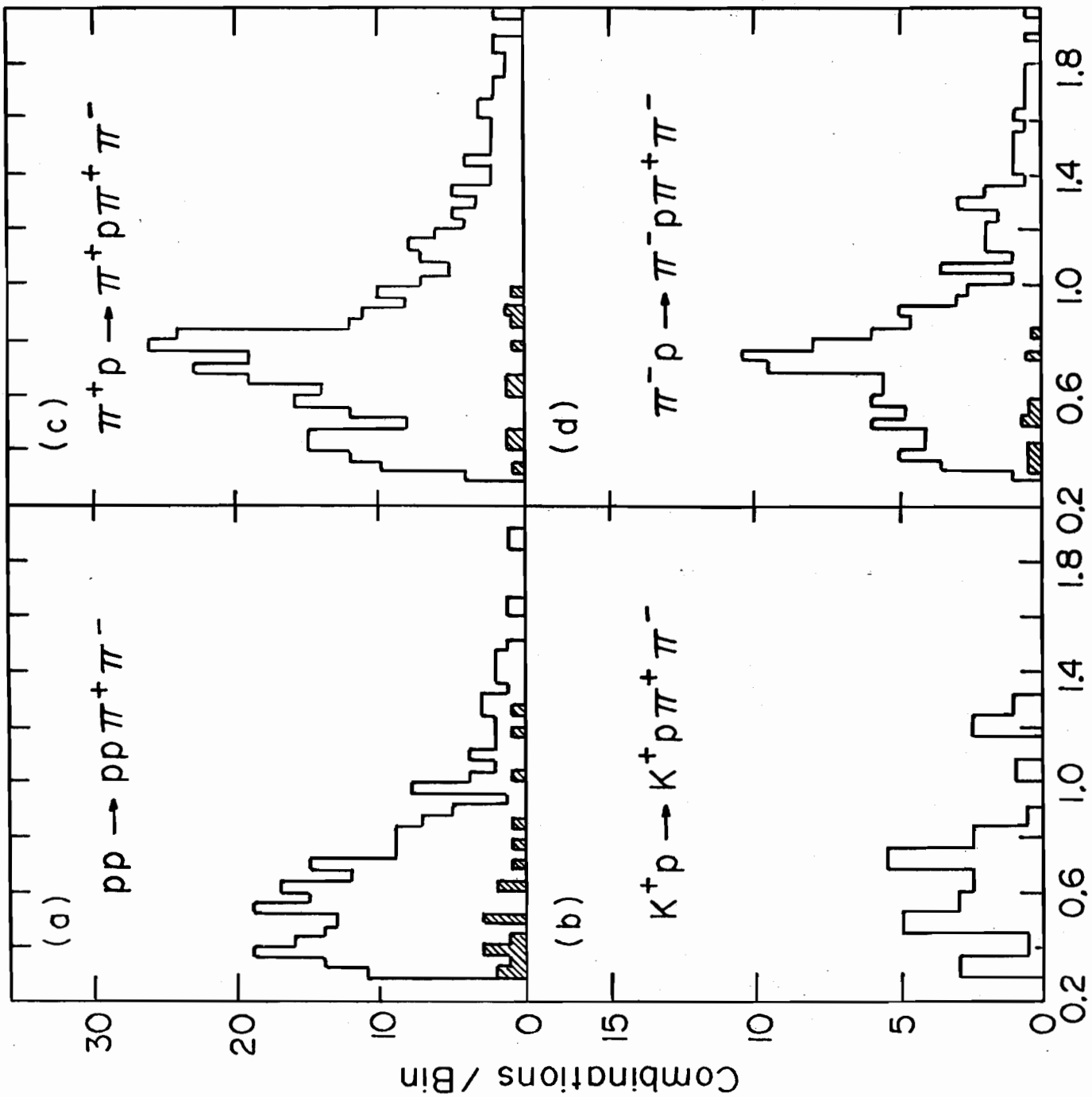
(a)
pp → ppπ⁺π⁻
(b)
K⁺p → K⁺pπ⁺π⁻
(c)
π⁺p → π⁺pπ⁺π⁻
(d)
π⁻p → π⁻pπ⁺π⁻
Combinations / Bin
M(π⁺ π⁻), GeV
0.2
0.6
1.0
1.4
1.8
0.2
0.6
1.0
1.4
1.8
0
5
10
15
0
10
20
30

Figure 5

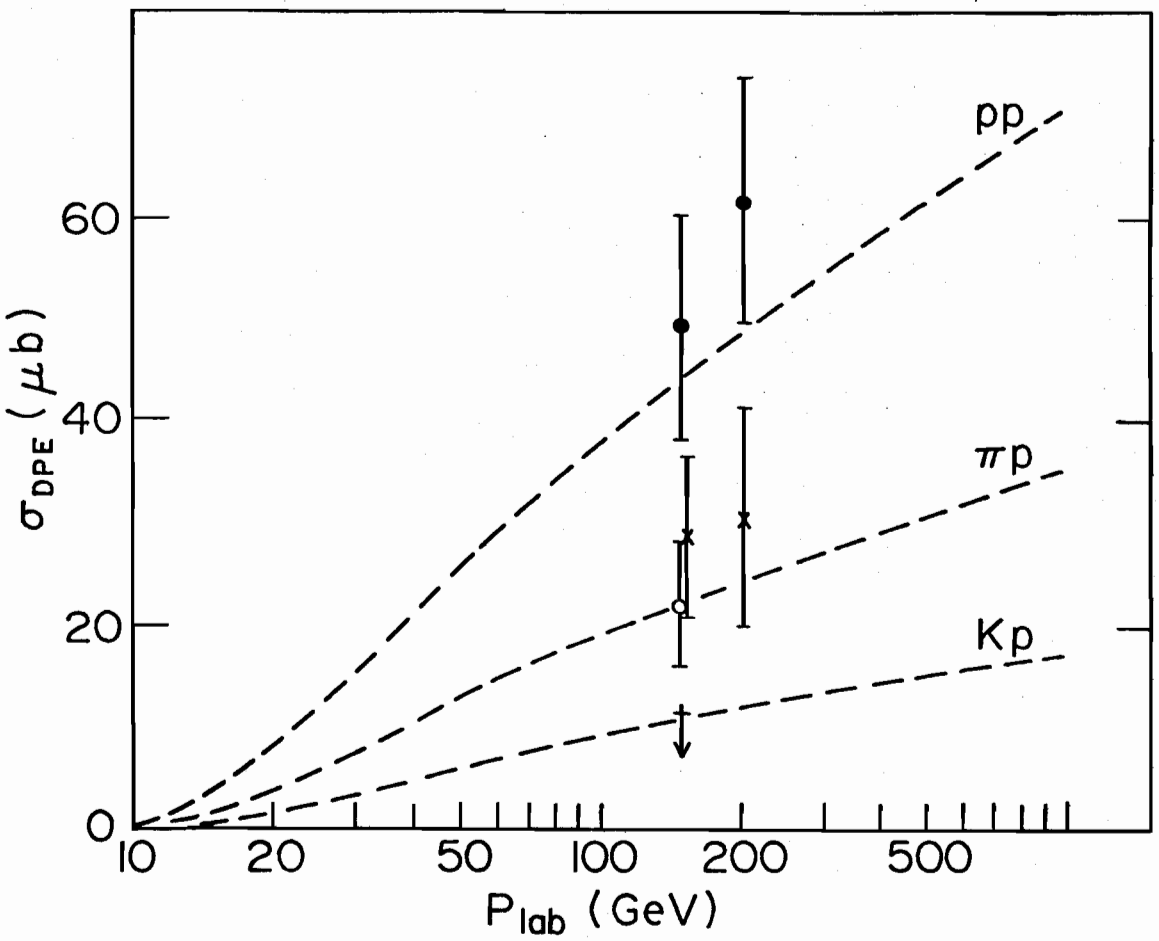
pp
πp
Kp
60
40
20
0
10
20
50
100
200
500
σ_{DPE} (μb)
P_{lab} (GeV)

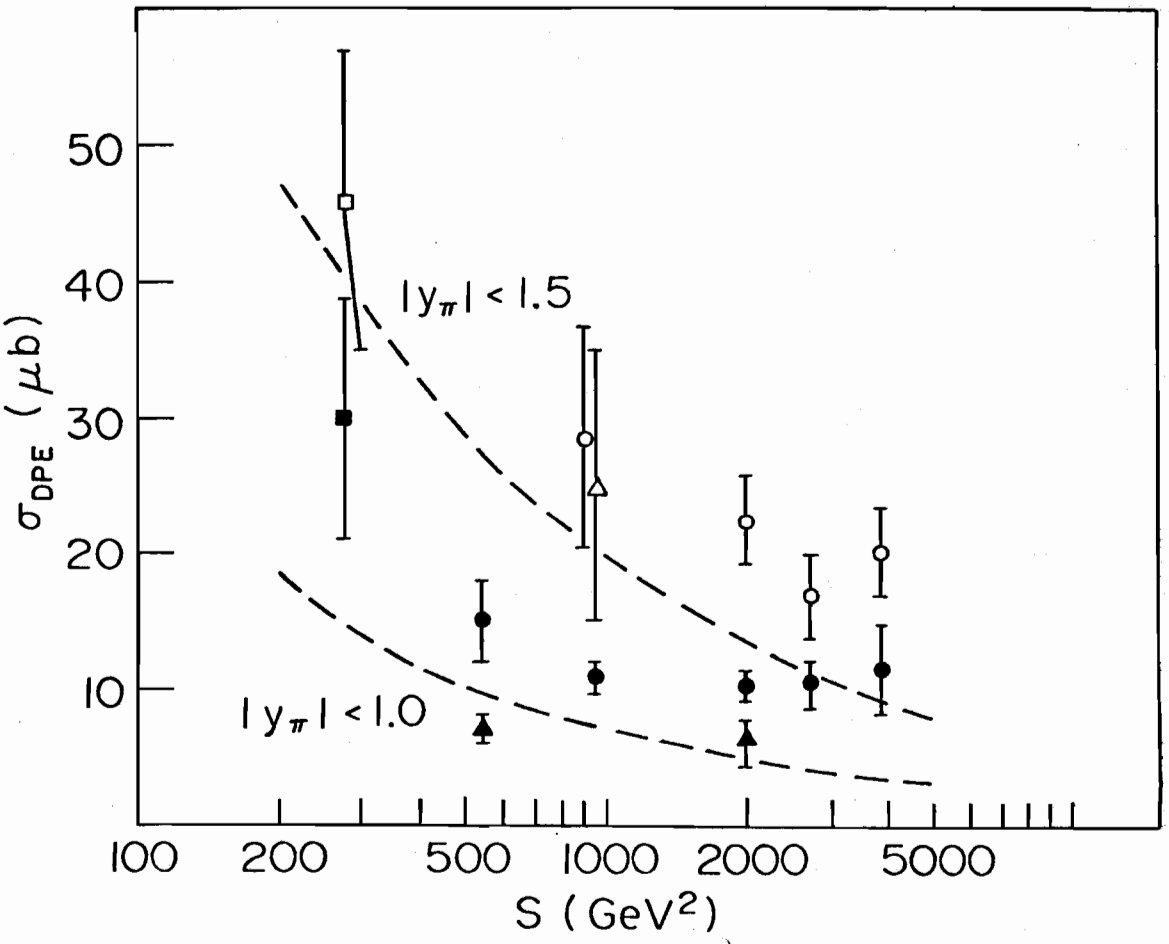
$|y_\pi| < 1.5$
$|y_\pi| < 1.0$
50
40
30
20
10
100
200
500
1000
2000
5000
σ_{DPE} (μb)
S (GeV²)

Figure 6

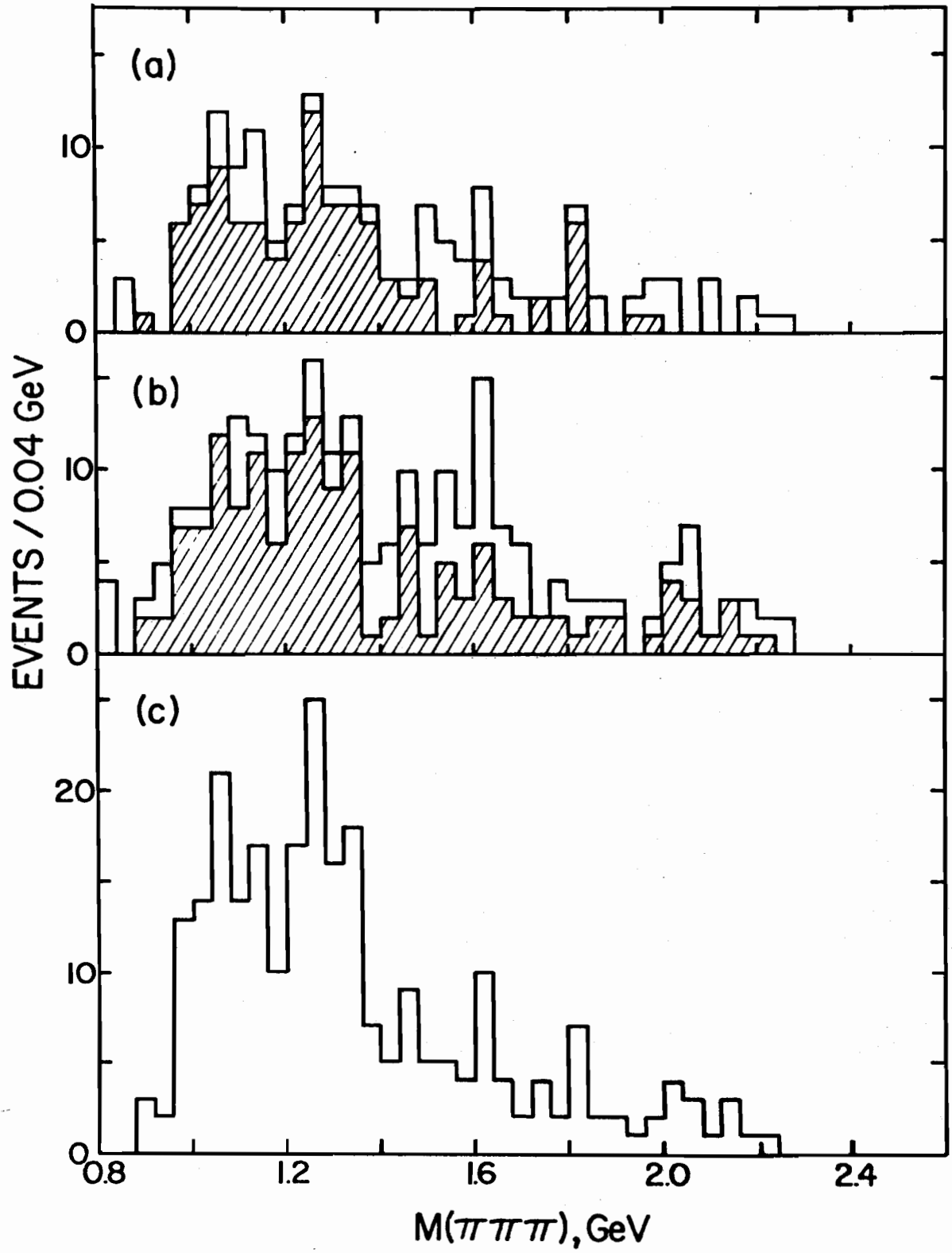

Figure 7

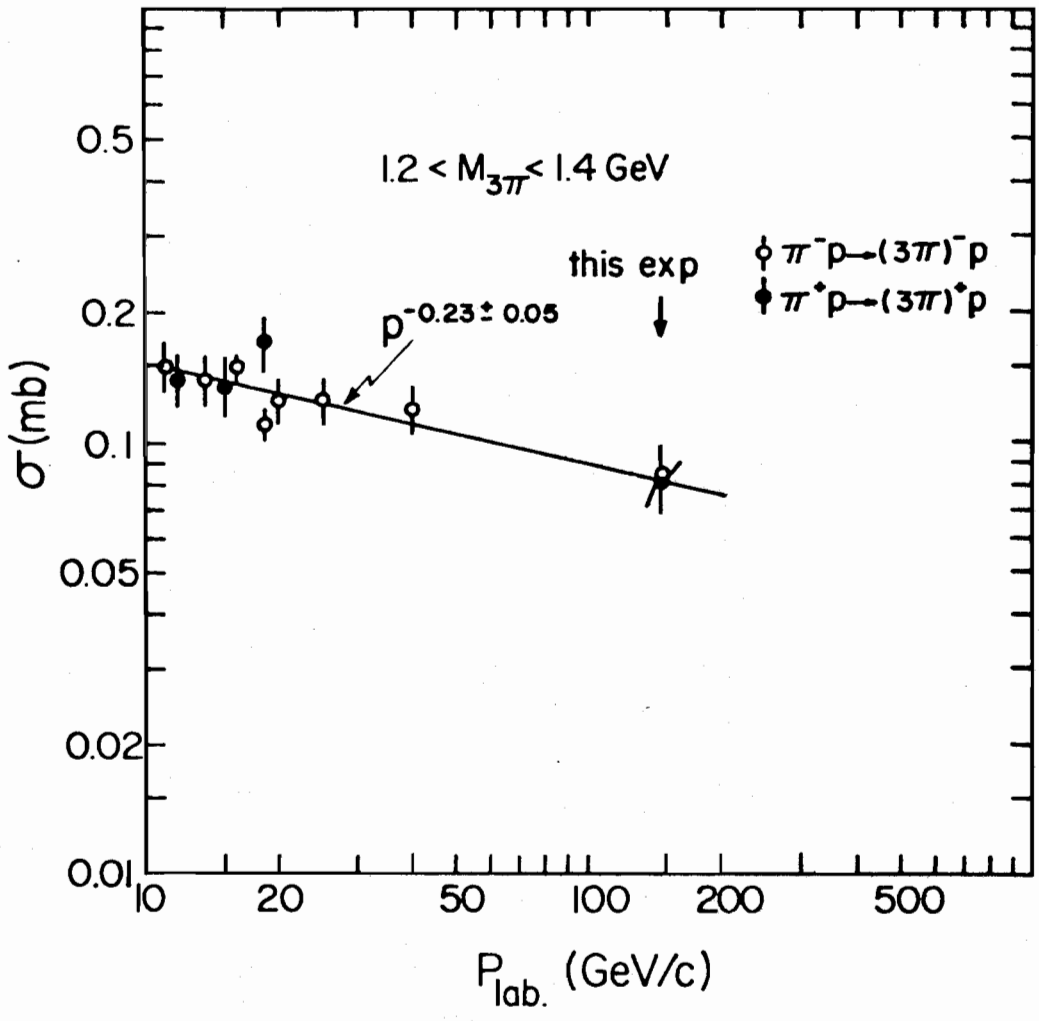
1.2 < M3π < 1.4 GeV
this exp
π⁻p→(3π)⁻p
π⁺p→(3π)⁺p
p^-0.23 ± 0.05
σ(mb)
0.5
0.2
0.1
0.05
0.02
0.01
10
20
50
100
200
500
P lab. (GeV/c)

Figure 8

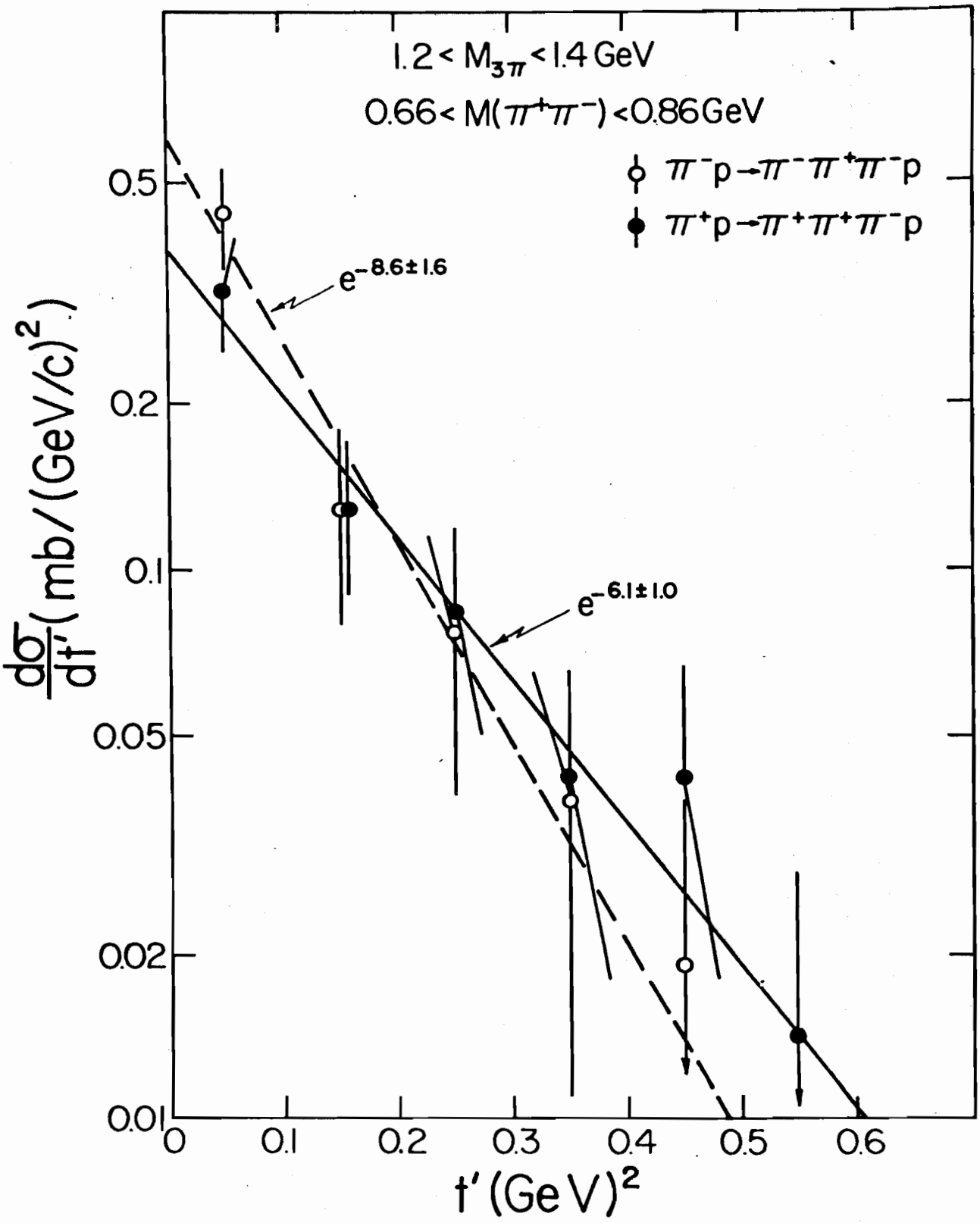
1.2 < M3π < 1.4 GeV
0.66 < M(π+π−) < 0.86 GeV
π−p → π−π+π−p
π+p → π+π+π−p
e−8.6±1.6
e−6.1±1.0
dσ/dt′ (mb/(GeV/c)²)
0.5
0.2
0.1
0.05
0.02
0.01
0
0.1
0.2
0.3
0.4
0.5
0.6
t′ (GeV)²

Figure 9